Journal of Physics: Conference Series **378** (2012) 012018 doi:10.1088/1742-6596/378/1/012018

Single Top quark production at lepton colliders

F. Peñuñuri[1], F. Larios[2] and Antonio O. Bouzas[2]

[1] Facultad de Ingeniería, Universidad Autónoma de Yucatán, A.P. 150, Cordemex, Mérida, Yucatan, México

[2] Departamento de Física Aplicada, CINVESTAV-Mérida, A.P. 73, 97310 Mérida, Yucatán, México

E-mail: larios@mda.cinvestav.mx

Abstract. Single top quark production at lepton (or non-hadronic) colliders like the e^+e^- International Linear Collider (ILC) can be used to obtain high precision measurements of the V_{tb} CKM matrix element as well as the effective tbW coupling. For the ILC we have calculated the QCD correction for the cross section in the context of an effective vector boson approximation. Our results show a $\sim 10\%$ increase due to the strong interaction.

1. Single Top production at e^+e^-, e^-e^-, γe and $\gamma\gamma$ colliders

The top quark is likely to provide us with the first clues of physics beyond the Standard Model [1]. The cross section for $t\bar{t}$ production being much greater than for single top has made this mode not only the one of initial discovery but also the one for further studies. In fact, new physics effects are probably already manifest in the recent $t\bar{t}$ forward-backward asymmetry observed at the Tevatron [2, 3]. On the other hand, single top production originates from the weak interaction and is directly proportional to the left handed tbW coupling. Just as it was at the Tevatron, in the LHC this process will be extensively studied [4].

The planned International Linear Collider (ILC) will collide electron and positron beams at an initial energy of 500 GeV and higher. It will provide a clean environment for the study of precision measurements. There are however other three possible modes of operation depending on the initial beams to be used like e^-e^-, γe and $\gamma\gamma$.

Table 1. Summary of results for the four types of lepton colliders studied in Ref. [5].

beams	Number of diagrams	$t\bar{t}$ background	σ(fb) ($\sqrt{s} = 0.5$ TeV)	σ(fb) ($\sqrt{s} = 1.0$ TeV)
$e^+\ e^-$	20	yes	3.1	6.7
$\gamma\gamma$	21	yes	9.2	18.8
$e\ e$	20	no	1.7	9.1
γe	4	no	30.3	67.6

The single top production processes at lepton and photon (e^+e^-, e^-e^-, γe and $\gamma\gamma$) colliders have been extensively studied at tree level in [5]. We can summarize their results in Table 1

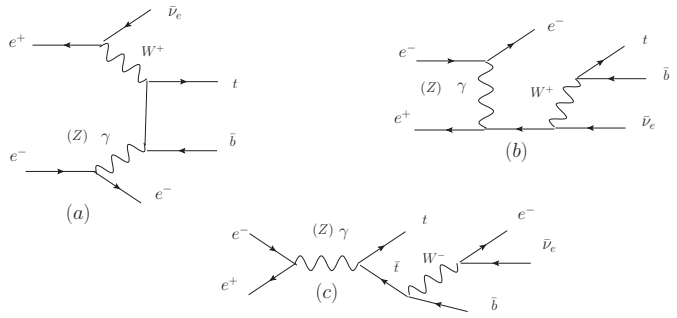

Figure 1. The three types of diagrams for the process $e^+e^- \to t\bar{b}e^-\bar{\nu}_e$: (a) vector boson fusion, (b) vector boson exchange and (c) e^+e^- annihilation.

where the four possible colliders are presented. The reaction $\gamma e^- \to \bar{t}b\nu_e$, is particularly suitable for precision studies, as it does not have the $t\bar{t}$ background. Compared to the ILC $e^+e^- \to t\bar{b}e^-\bar{\nu}_e$ process the γe^- reaction can yield a larger production rate and is directly proportional to the V_{tb} term. Further studies have thus been done for this reaction. In particular, the QCD corrections have been studied in [6]. Their conclusion is that the QCD correction is not very large ($\sim 5\%$) so that this mode remains very well suited for a precise measurement of V_{tb}. The approach of [6] is to use the effective vector boson approximation, or *effective W approximation* [7] (EWA) and to compute the QCD loop corrections for the $W^+\gamma \to t\bar{b}$ fusion process. Then, the convolution with the $f_{W^+/e^+}(x)$ distribution function is applied to obtain the correction to the actual $e^+\gamma$ process. We would like to point out that the authors of [6] have made a very clear and thorough presentation of the calculation. In this work we use their analysis of the $W^+\gamma \to t\bar{b}$ process to estimate the QCD correction for the $e^+e^- \to t\bar{b}e^-\bar{\nu}_e$ process of the ILC. Here, in addition to the convolution with the W^+ boson distribution function we will use the effective photon (as well as the effective Z boson) approximation to obtain the QCD correction. We will use the same input values as in [6] for masses and coupling constants, except for the masses of top and bottom quarks we take $m_t = 173$ GeV and $m_b = 4.2$ GeV.

2. Vector boson contributions at tree level

At tree level there are 20 diagrams for the process $e^+e^- \to t\bar{b}e^-\bar{\nu}_e$ [5]. We can list them in three different types: (a) vector boson fusion, (b) vector boson exchange and (c) e^+e^- annihilation (see Figure1). For the energy range we consider one of the diagrams actually corresponds to $t\bar{t}$ production, where one of the tops decays leptonically. In order to exclude $t\bar{t}$ production from the single top process we discard all events where the invariant mass of the decay products (e^-,$\bar{\nu}_e$,$\bar{b}$) falls inside an interval around the top mass $m_t - \Delta M \leq M_{e\nu b} \leq m_t + \Delta M$. We take the value $\Delta M = 20$GeV as in [5].

The effective W approximation relies on the fact that the vector boson fusion diagrams become dominant when heavy particles are produced in very high energy collisions [7]. In general, three conditions should be met for the EWA to work well: (1) The mass of the vector boson (M_W or M_Z) should be much smaller than its energy, and this can be met if we require $M_V \ll \sqrt{s}/2$, (2) For $q\bar{q}$ production $m_q \gg M_V$, this is true for the top quark but not for the bottom quark, and (3) One polarization mode should be dominant so that interference effects can be neglected. Fortunately, in our case the mode $W\gamma \to t\bar{b}$ dominates for longitudinal W, and the modes with the Z boson $WZ \to t\bar{b}$ give even lower contributions.

As expected, this method works very well for $t\bar{t}$ production at high $\sqrt{s}$ and to a lesser degree for single top, which in our case can be seen as $t\bar{b}$ production. In [6] the QCD correction to the

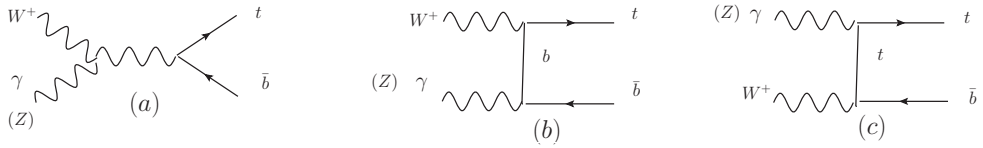

Figure 2. Diagrams for the $W^+\gamma(Z) \to t\bar{b}$ process.

process $e^+\gamma \to t\bar{b}\bar{\nu}_e$ was calculated by doing first the QCD correction to the $W^+\gamma$ fusion into $t\bar{b}$ and then by taking the convolution with an effective W^+ coming from the initial positron (see Figure 2). We follow the same approach by doing the one loop QCD correction to $W^+\gamma \to t\bar{b}$ as well as $W^+Z \to t\bar{b}$ and then convoluting with the effective distribution functions for W^+, γ and Z:

$$\begin{aligned}\sigma(e^+e^- \to t\bar{b}\bar{\nu}_e e^-) \quad &= \quad (1)\\ &\sum_{W_L,W_T} \int_{x_W^{\min}}^1 dx_W f_{W^+/e^+}(x_W) \int_0^1 dx_\gamma f_{\gamma/e^-}(x_\gamma)\, \sigma(W^+\gamma \to t\bar{b})(\hat{s})\\ + \quad &\sum_{W_{L,T},Z_{L,T}} \int_{x_W^{\min}}^1 dx_W f_{W^+/e^+}(x_W) \int_{x_Z^{\min}}^1 dx_Z f_{Z/e^-}(x_Z)\, \sigma(W^+Z \to t\bar{b})(\hat{s})\end{aligned}$$

Where, $x_V^{\min} = 2M_V/\sqrt{s}$, $\hat{s} = x_W x_\gamma s$ or $x_W x_Z s$, and the structure functions can be found in [7]. The tree-level cross section for single top production at the ILC is shown in Fig. 3. The exact Born-level calculation for the $e^+e^- \to t\bar{b}e^-\bar{\nu}_e$ process is obtained with CalcHEP [8] and is shown by the solid line. We can see that the prediction of the EWA (dot-dashed curve) is in very good agreement with the exact result for center of mass energies above 1.5 TeV. However, for the energy range of the ILC the EWA values can be significantly lower. In particular, for $\sqrt{s} = 1000$GeV there is a 15% difference and for $\sqrt{s} = 500$GeV the EWA result is about one half of the exact value.

Some kinematical aspects of our calculation are worth discussing in more detail. Because in the dominant diagrams for the complete process $e^+e^- \to W^{+*}Z^* \to t\bar{b}e^-\bar{\nu}_e$ the virtual vector bosons get space-like momenta $k_V^2 \leq 0$ ($V = W$, Z) and are always far from their mass shell, the EWA is known to work better when the vector-boson squared momenta are set to $k_V^2 = 0$ in the external legs, as discussed in [10]. Nevertheless, when dealing with a process like $t\bar{t}$ production one may set $k_V^2 = M_V^2$, as this introduces only a small error of order $M_V/\sqrt{s}$. For this reason it is customary [7, 6] to set the external massive W^+ and Z on-shell for convenience. We stress here, however, that the EWA requires [7, 10] the limits of integration to be taken as defined in (1) for all polarization states of the massive vector bosons, regardless of whether one chooses to set $k_V^2 = 0$ or M_V^2 [1]. In our study we keep the EWA condition $k_Z^2 = 0$ for the Z boson, but choose $k_W^2 = M_W^2$ for the initial-state W^+ for calculational convenience. We have numerically checked that indeed by setting $k_W^2 = 0$ we don't find a significant change in the result.

Because of the kinematics of the $W^+Z \to t\bar{b}$ process, its tree-level scattering amplitude has a pole singularity within its physical region [9], leading to divergent behavior as we integrate it over the Mandelstam variable t (or the polar angle of the outgoing quark). This is due to the fact that, for energy values from slightly above the threshold $m_t + m_b$ and up to ~ 3 TeV, there exists a certain value of t such that the massive Z boson can actually decay into $b\bar{b}$, causing the bottom quark propagator to hit its pole at that t. By strictly adhering to the EWA requirement $k_Z^2 = 0$,

[1] Notice that in [6] the lower limit is set to $x_W^{\min} = 0$ for the longitudinal W^+ distribution, a procedure that is only justified a posteriori by their results.

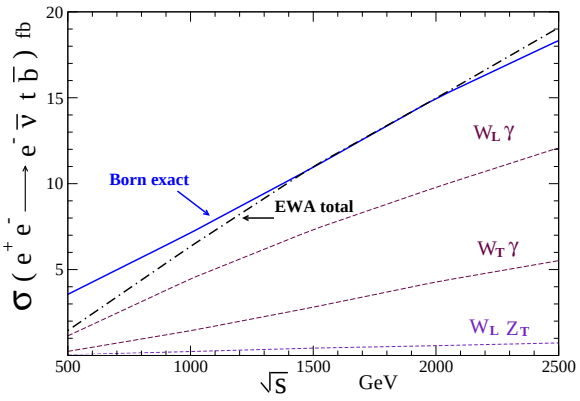

Figure 3. The Born cross section for single top production at the ILC.

the singularity is pushed outside the physical region and no divergent integration appears in the computation. Notice that a similar situation does not occur with the W^+ boson, as it cannot decay into $t\bar{b}$.

Below, we will describe the QCD corrections to the $W^+\gamma$ and W^+Z processes, including the Dipole Subtraction Method of infrared divergences. We have followed closely the analysis of the $W^+\gamma$ mode done by Kuhn et.al. in [6].

3. QCD correction to the $W^+\gamma(Z) \to t\bar{b}$ process.

The QCD loop correction to the $W^+\gamma(Z) \to t\bar{b}$ process is given by 9 Feynman diagrams (see Fig.2 of [6]). The renormalization procedure involves only the quark's wave function and mass parameter. Specific formulas can be found in [6]. Concerning the renormalization scale dependence we have also set α_s at the scale $\mu = \sqrt{s}$ for our numerical calculation (it becomes $\sqrt{\hat{s}}$ under the convolution). The extraction of IR singularities is done with the subtraction method of the dipole formalism [11]. This method consists of adding and subtracting a so-called dipole term:

$$\sigma^{NLO}(W^+\gamma \to t\bar{b}) = \int_{tbg} \left[(d\sigma^R)_{\epsilon=0} - (d\sigma^B \otimes dV_{dipole})_{\epsilon=0}\right] + \int_{tb} [d\sigma^V + d\sigma^B \otimes \mathbf{I}]_{\epsilon=0} \qquad (2)$$

Where $d\sigma^R$ comes from the real emission $W^+\gamma(Z) \to t\bar{b}g$ process and $d\sigma^B \otimes dV_{dipole}$ is the subtracting dipole term that matches pointwise the singularities associated with the soft and/or collinear gluon. Both terms are calculated in $d = 4$ dimensions. In the second integral the same dipole term has been partially integrated in the gluon phase space and then added to the virtual correction $d\sigma^V$. This sum is performed in $d = 4 - 2\epsilon$ dimensions (consistent with dimensional regularization).

The general formula for the dipole term is found in Eq. (5.16) of [11]. The specific expression in our case is:

$$d\sigma^B \otimes dV_{dipole} \quad = \frac{\langle V_{gt,b}\rangle}{2k_g \cdot k_t} |\mathcal{M}_0(\tilde{k}_{gt}, \tilde{k}_b)|^2 \; + \; \{t \leftrightarrow b\}\,, \qquad (3)$$

where

$$\langle V_{gt,b}\rangle \quad = 8\pi\alpha_s C_F \{\frac{2}{1 - \tilde{z}_t(1 - y_{gt,b})} - \frac{\tilde{v}_{gt,b}}{v_{gt,b}}[1 + \tilde{z}_t + \frac{m_t^2}{k_g \cdot k_t}]\}\,,$$

$$
\begin{aligned}
\tilde{z}_t &= \frac{k_t\cdot k_b}{(k_t+k_g)\cdot k_b}\,, \qquad y_{gt,b} = 2\frac{k_g\cdot k_t}{s x_{tb}}\,, \qquad \tilde{v}_{gt,b} = \frac{\lambda_{tb}}{x_{tb}}\,,\\
v_{gt,b} &= \sqrt{(1+a_{gt,b})^2 - a_{gt,b}^2/z_b}\,, \qquad a_{gt,b} = \frac{2z_b}{x_{tb}(1-y_{gt,b})}\,,\\
\tilde{k}_b &= \frac{x_b}{2}P + \frac{\lambda_{tb}}{\lambda_{gt}}(k_b - \frac{P\cdot k_b}{s}P)\,, \qquad \tilde{k}_{gt} = P - \tilde{k}_b\,, \qquad P = k_W + k_\gamma\,,
\end{aligned}
$$

and $\mathcal{M}_0(\tilde{k}_{gt},\tilde{k}_b)$ is the Born-level $W^+\gamma\to t\bar{b}$ amplitude with one modification: the final state momenta k_t and k_b have been replaced by $\tilde{k}_{gt}$ and $\tilde{k}_b$ respectively. The other variables are defined as in [6]: $\mu_q = m_q/\sqrt{s}$, $z_q = \mu_q^2$, $x_t = 1+z_t-z_b$, $x_b = 1+z_b-z_t$, $x_{tb} = 1-z_t-z_b$, $\lambda_{tb} = \lambda(1,z_t,z_b)$, $\lambda_{gt} = \lambda(1,(k_g+k_t)^2/s,z_b)$, and $\lambda(x,y,z) = \sqrt{x^2+y^2+z^2-2xy-2xz-2yz}$.

For the real emission correction we have prepared a Fortran program that integrates the cross section for the $W^+\gamma\to t\bar{b}g$ process along with dipole subtraction. As it turns out, the subtraction term defined by the dipole formalism in the first integral of Eq. (2) is actually a very good approximation to the real emission cross section in an important part of the *tbg* phase space, so that the numerical results we obtained were very small: about two orders of magnitude below the values obtained for the virtual correction.

The expression for the dipole term in the virtual correction is:

$$
d\sigma^B\otimes\mathbf{I} = |\mathcal{M}_d(W^+\gamma\to t\bar{b})|^2\frac{\alpha_s}{2\pi}\frac{1}{\Gamma(1-\epsilon)}\left(\frac{4\pi\mu^2}{s}\right)^{\epsilon}(\mathbf{I}_{gt,b}+\mathbf{I}_{gb,t})\,, \tag{4}
$$

where $\mathcal{M}_d(W^+\gamma\to t\bar{b})$ is the Born-level amplitude in $d=4-2\epsilon$ dimensions (the flux term of the $t\bar{b}$ phase space integration is understood). The dipole function is given by $\mathbf{I}_{gt,b} = C_F[2I^{eik}+I^{coll}_{gt,b}]$ (also $\mathbf{I}_{gb,t} = \mathbf{I}_{gt,b}\{t\leftrightarrow b\}$), where I^{eik} and $I^{coll}_{gt,b}$ are given by Eqs. (5.34) and (5.35) in [11]:

$$
\begin{aligned}
I^{eik} &= \frac{x_{tb}}{\lambda_{tb}}\{\frac{\ln\rho}{2\epsilon}+\frac{\pi^2}{6}-\ln\rho\ln[1-(\mu_t+\mu_b)^2]-\frac{1}{2}ln^2\rho_t-\frac{1}{2}ln^2\rho_b\\
&\quad +2Li_2(-\rho)-2Li_2(1-\rho)-\frac{1}{2}Li_2(1-\rho_t^2)-\frac{1}{2}Li_2(1-\rho_b^2)\}\\
I^{coll}_{gt,b} &= \frac{1}{\epsilon}+3+\ln\mu_t+\ln(1-\mu_b)-2\ln[(1-\mu_b)^2-z_t]-\frac{\mu_b}{1-\mu_b}\\
&\quad -\frac{2}{x_{tb}}\left[\mu_b(1-2\mu_b)+z_t\ln\frac{\mu_t}{1-\mu_b}\right]
\end{aligned} \tag{5}
$$

where $\rho^2 = (x_{tb}-\lambda_{tb})/(x_{tb}+\lambda_{tb})$, $\rho_t = (x_{tb}-\lambda_{tb}+2z_t)/(x_{tb}+\lambda_{tb}+2z_t)$, and $\rho_b = \rho_t\{t\leftrightarrow b\}$. These formulas also appear in [6], except that in their Eq. (4.14) in $I^{coll}_{gt,b}$ the constant term should not be 5 but 3.

Concerning the calculation of $d\sigma^V$, the details can be found in [6]. We actually worked out this same computation before doing the case for the Z boson. As expected from the results shown in Fig. 3 the contribution from W^+Z fusion is much smaller than the one from $W^+\gamma$. In fact, we only considered the correction for the polarizations W^+ longitudinal and Z transversal as the other possibilities yield negligible contributions.

Our results are shown in Figs. 4 and 5. The solid line in Fig. 4 is the same exact Born-level result shown in Fig. 3. The dashed line is obtained by adding to the solid line the QCD correction computed within the EWA method. Fig. 5 shows the ratio of the QCD correction to the exact Born cross section (solid line). As seen there, for $\sqrt{s} > 1$ TeV the QCD correction remains roughtly stable about 11%. Its slow decrease above ~ 2 TeV is due to the running of $\alpha_s(\mu=\sqrt{\hat{s}})$. On the other hand, below 1 TeV the correction drops to 7% with decreasing

energy. This is an effect of the Born-level EWA predicted cross section, that drops to $\sim 50\%$ of the exact Born-level value as shown in Fig. 3. If instead of using the exact Born value as denominator we use the EWA Born prediction (see dot-dashed line in Fig. 3) our results (dashed line) show a 17% increase in the Born level cross section at $\sqrt{s} = 500$ GeV.

It will be interesting to compare this result based on the effective W approximation with a future more robust calculation based on the complete $e^+e^- \to t\bar{b}e^-\bar{\nu}_e$ process.

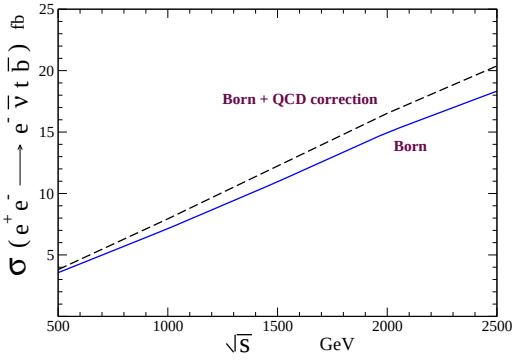

Figure 4. The QCD correction from $W^+\gamma$ and W^+Z fusion to the $e^+e^- \to t\bar{b}e^-\bar{\nu}_e$ process. The exact Born-level calculation (solid line) and Born plus QCD correction (dashed line).

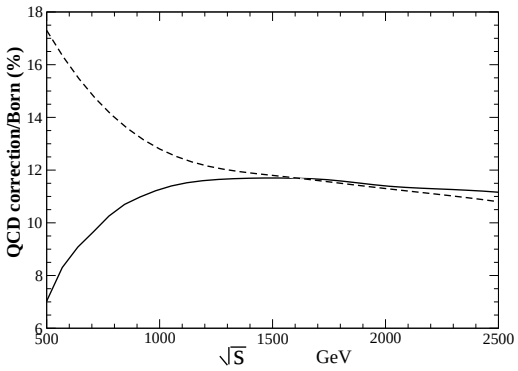

Figure 5. Ratio of QCD correction to exact Born cross section (solid line) and ratio of QCD correction to EWA Born cross section (dashed line).

Acknowledgments
We thank RedFAE, Conacyt and SNI for support. F.L. thanks C.-P. Yuan for useful discussions.

References

[1] Kumar K, Tait TMP and Vega-Morales R 2009, *JHEP* **0905**, 022; Berger EL, Cao QH and Low I 2009, *Phys. Rev.* D**80**, 074020; Bernreuther W, Gonzalez P and Wiebusch M 2009, *Eur. Phys. J.* C**60**, 197; del Aguila F, Aguilar-Saavedra J, Moretti M, Piccinini F, Pittau R and Treccani M 2010, *Phys. Lett.* B**685**, 302; Liu GL 2010, *Phys. Rev.* D**82**, 115032; Cakir IT, Cakir O and Sultansoy S 2010, *Phys. Lett.* B**685**, 170; Zhang C and Willenbrock S 2011, *Phys. Rev.* D**83**, 034006; Groote S, Korner JG, Melic B and Prelovsek S 2011, *Phys. Rev.* D**83** 054018; Martinez R, Perez MA and Poveda N 2008, *Eur. Phys. J.* C**53**, 221-230; Cordero-Cid A, Perez MA, Tavares-Velasco G *et al.* 2004, *Phys. Rev.* D**70**, 074003.

[2] Abazov VM *et al.* [D0 Collaboration] 2008, *Phys. Rev. Lett.* **100**, 142002; Aaltonen T *et al.* [CDF Collaboration] 2008, *Phys. Rev. Lett.* **101**, 202001; *ibid* 2011 *Phys. Rev.* D**83** 112003.

[3] Chivukula RS, Simmons EH and Yuan CP 2010, *Phys. Rev.* D**82**, 094009; Shu J, Tait TMP and Wang K 2010, *Phys. Rev.* D**81**, 034012; Berger EL, Cao QL, Chen CR, Li CS and Zhang H 2011, *Phys. Rev. Lett.* **106** 201801; Cao J, Wang L, Wu L and Yang JM 2011, *Phys. Rev.* D**84** 074001.

[4] Heim S, Cao Q. -H., Schwienhorst R and Yuan C.-P. 2010 *Phys. Rev.* D**81**, 034005; Cao Q. -H., Schwienhorst R, Benitez J. A. and Yuan C.-P. 2005, *Phys. Rev.* D**72**, 094027; Cao Q. -H., Schwienhorst R and Yuan C. -P. 2005, *Phys. Rev.* D**71**, 054023; Campbell J. M., Frederix R, Maltoni F and Tramontano F 2009, *Phys. Rev. Lett.* **102**, 182003; Kidonakis N 2010, *Phys. Rev.* D**81**, 054028; Falgari P, Mellor P and Signer A 2010, *Phys. Rev.* D**82**, 054028; Wang J, Li CS, Zhu HX and Zhang JJ 2010, *Preprint* hep-ph/1010.4509; Barger V, McCaskey M and Shaughnessy G 2010, *Phys. Rev.* D**81**, 034020; Bordes G and van Eijk B 1995, *Nucl. Phys.* B**435** 23; Smith MC and Willenbrock S 1996, *Phys. Rev.* D**54** 6696; Stelzer T, Sullivan Z and Willenbrock S 1997, *Phys. Rev.* D**56** 5919; B.W. Harris et al 2002, *Phys. Rev.* D**66** 054024.

[5] Boos E et al. 2001, *Eur. Phys. J.* C**21**, 81.

[6] Kuhn JH, Sturm C and Uwer P 2003, *Eur. Phys. J.* C**30**, 169.

[7] Dawson S 1985, *Nucl. Phys.* B249, 42.

[8] A.Pukhov et al 1999, *Preprint* hep-ph/9908288; A.Pukhov 2004 *Preprint* hep-ph/0412191.

[9] Coleman S and Norton RE 1965, *Nuov. Cim.* **38** 438.

[10] Kauffman R 1989, Ph.D. thesis, SLAC-0348.

[11] Catani S, Dittmaier S, Seymour MH and Trocsanyi Z 2002, *Nucl. Phys.* B**627**, 189.